

## Supporting Information

Novel magnetic Fe-Ti-V spinel catalyst for the selective catalytic reduction of NO with NH<sub>3</sub> in a broad temperature range

Shijian Yang,<sup>a,b</sup> Chizhong Wang,<sup>a</sup> Jinghuan Chen,<sup>a</sup> Yue Peng,<sup>a</sup> Lei Ma,<sup>a</sup> Huazhen Chang,<sup>a</sup> Liang Chen,<sup>a</sup> Caixia Liu,<sup>a</sup> Jiayu Xu,<sup>a</sup> Junhua Li,<sup>\*a</sup> and Naiqiang Yan <sup>\*b</sup>

<sup>a</sup> *School of Environment, Tsinghua University, Haidian District, Beijing, 100084 P. R. China*

<sup>b</sup> *School of Environmental Science and Engineering, Shanghai Jiao Tong University, 800 Dong Chuan Road, Shanghai, 200240 P. R. China*

## 1. Experimental

### 1.1 Catalyst preparation

Nanosized  $\text{Fe}_{2.5}\text{Ti}_{0.5}\text{O}_4$ ,  $\text{Fe}_2\text{Ti}_{0.5}\text{Mn}_{0.5}\text{O}_4$  and  $\text{Fe}_2\text{Ti}_{0.5}\text{V}_{0.5}\text{O}_4$ , the precursors of  $(\text{Fe}_{2.5}\text{Ti}_{0.5})_{1-\delta}\text{O}_4$  (Fe-Ti spinel),  $(\text{Fe}_2\text{Ti}_{0.5}\text{Mn}_{0.5})_{1-\delta}\text{O}_4$  (Fe-Ti-Mn spinel) and  $(\text{Fe}_2\text{Ti}_{0.5}\text{V}_{0.5})_{1-\delta}\text{O}_4$  (Fe-Ti-V spinel), were prepared using a co-precipitation method at room temperature.<sup>1, 2</sup> Suitable amounts of ferrous sulfate, ferric trichloride, titanium tetrachloride and vanadyl dichloride (or manganese sulfate) were dissolved in a HCl solution. This mixture was added to an ammonia solution leading to an instantaneous precipitation. During the reaction, the system was continuously stirred at 800 rpm. The particles were then separated by centrifugation at 4500 rpm for 5 min and washed with distilled water followed by a new centrifugation. After 4 washings, the particles were collected and dried in a vacuum oven at 105 °C for 12 h.  $(\text{Fe}_{2.5}\text{Ti}_{0.5})_{1-\delta}\text{O}_4$ ,  $(\text{Fe}_2\text{Ti}_{0.5}\text{Mn}_{0.5})_{1-\delta}\text{O}_4$  and  $(\text{Fe}_2\text{Ti}_{0.5}\text{V}_{0.5})_{1-\delta}\text{O}_4$  were obtained after the thermal treatment of  $\text{Fe}_{2.5}\text{Ti}_{0.5}\text{O}_4$ ,  $\text{Fe}_2\text{Ti}_{0.5}\text{Mn}_{0.5}\text{O}_4$  and  $\text{Fe}_2\text{Ti}_{0.5}\text{V}_{0.5}\text{O}_4$  under air at 400 °C for 3 h, respectively.

Meanwhile, conventional vanadium-based catalyst ( $\text{V}_2\text{O}_5\text{-WO}_3/\text{TiO}_2$ ) was prepared as a comparison.  $\text{V}_2\text{O}_5\text{-WO}_3/\text{TiO}_2$  catalysts with 10 wt.%  $\text{V}_2\text{O}_5$  and 10 wt.%  $\text{WO}_3$ , and 1 wt. %  $\text{V}_2\text{O}_5$  and 10 wt.%  $\text{WO}_3$  were prepared by the conventional impregnation method using  $\text{NH}_4\text{VO}_3$ ,  $(\text{NH}_4)_{10}\text{W}_{12}\text{O}_{41}$  and  $\text{H}_2\text{C}_2\text{O}_4\cdot2\text{H}_2\text{O}$  as precursors, and anatase  $\text{TiO}_2$  as support. After the impregnation, excess water was removed in a rotary evaporator at 80 °C. The sample was dried at 100 °C overnight and then calcined at 550 °C for 3 h under air.

### 1.2 Catalyst characterization

Crystal structure was determined using an X-ray diffractionmeter (Rigaku, D/max-2200/PC) between 20° and 70° at a step of 7° min<sup>-1</sup> operating at 30 kV and 30 mA using Cu K $\alpha$  radiation. BET surface area was determined using a nitrogen adsorption apparatus (Quantachrome, Autosorb-1). Catalyst was outgassed at 200 °C before BET measurement. Saturated magnetization was determined using a vibrating sample magnetometer (VSM, Model JDM-13) at room temperature. X-ray photoelectron spectroscopy (XPS, Thermo ESCALAB 250) was used to determine the Fe 2p, V 2p, Mn 2p, Ti 2p and O 1s binding energies with Al K $\alpha$  ( $\text{h}\nu=1486.6$  eV) as the excitation source. The C 1s line at 284.6 eV was taken as a reference for the binding energy calibration.

### 1.3 Catalytic test

SCR reaction was performed on a fixed-bed quartz tube reactor (6 mm of internal diameter) containing 100-200 mg of catalyst (40-60 mesh). The typical reactant gas composition was as follows: 500 ppm of NO, 500 ppm of NH<sub>3</sub>, 2% of O<sub>2</sub>, and balance of N<sub>2</sub>. The total flow rate ranged from 100 to 200 mL min<sup>-1</sup>, and the gas hourly space velocity (GHSV) varied from about 37500 to 150000 h<sup>-1</sup>. The concentrations of NO and NO<sub>2</sub> were continually monitored by a chemiluminescent NO/NO<sub>x</sub> analyzer (Thermo, Model 42*i*-HL). Meanwhile, the concentrations of NH<sub>3</sub> and N<sub>2</sub>O were continually monitored by a FTIR spectrometer (Gasmet FTIR DX4000).

As the SCR reaction reached the steady state, the ratios of NO conversion and N<sub>2</sub> selectivity were calculated according to the following equations:

$$\text{NO conversion \%} = \frac{[\text{NO}]_{\text{in}} - [\text{NO}]_{\text{out}}}{[\text{NO}]_{\text{in}}} \times 100\% \quad (1)$$

$$\text{N}_2 \text{ selectivity \%} = 1 - \frac{2[\text{N}_2\text{O}]_{\text{out}} + [\text{NO}_2]_{\text{out}}}{[\text{NO}]_{\text{in}} - [\text{NO}]_{\text{out}} + [\text{NH}_3]_{\text{in}} - [\text{NH}_3]_{\text{out}}} \times 100\% \quad (2)$$

### 1.4 In situ DRIFTS study

In situ DRIFT spectra were recorded on a Fourier transform infrared spectrometer (FTIR, Nicolet NEXUS 870) equipped with a smart collector and an MCT detector cooled by liquid N<sub>2</sub>. The diffuse reflectance measurement was carried out in situ in a high temperature cell with a ZnSe window. The FTIR spectra were recorded by accumulating 100 scans with a resolution of 4 cm<sup>-1</sup>.

## 2. Characterization results

### 2.1 XRD

XRD patterns of (Fe<sub>2.5</sub>Ti<sub>0.5</sub>)<sub>1-δ</sub>O<sub>4</sub>, (Fe<sub>2</sub>Ti<sub>0.5</sub>Mn<sub>0.5</sub>)<sub>1-δ</sub>O<sub>4</sub> and (Fe<sub>2</sub>Ti<sub>0.5</sub>V<sub>0.5</sub>)<sub>1-δ</sub>O<sub>4</sub> are shown in Fig. S1. The characteristic reflections of (Fe<sub>2.5</sub>Ti<sub>0.5</sub>)<sub>1-δ</sub>O<sub>4</sub> corresponded very well to the standard card of maghemite (JCPDS: 39-1346). If there were some amorphous TiO<sub>2</sub> in synthesized Fe<sub>2.5</sub>Ti<sub>0.5</sub>O<sub>4</sub>, it should transform to rutile (or anatase) after the calcination at 400 °C for 3 h.<sup>3</sup> As shown in Fig. S1a, the characteristic peaks corresponding to rutile and anatase did not appear. Furthermore, the lattice parameter of (Fe<sub>2.5</sub>Ti<sub>0.5</sub>)<sub>1-δ</sub>O<sub>4</sub> was bigger than that of pure phase γ-Fe<sub>2</sub>O<sub>3</sub> (0.8351 nm) because the radius of Ti<sup>4+</sup> (0.68 Å) is bigger than that of Fe<sup>3+</sup> (0.64 Å). They both suggest Ti was introduced into the spinel structure.

After the further incorporation of Mn into the spinel structure, additional peaks that would indicate the presence of other crystalline manganese oxides, such as  $\text{Mn}_3\text{O}_4$  (hausmannite),  $\text{Mn}_2\text{O}_3$  (bixbyite) or  $\text{MnO}_2$ , were not present in the diffraction scan of  $(\text{Fe}_2\text{Ti}_{0.5}\text{Mn}_{0.5})_{1-\delta}\text{O}_4$  (shown in Fig. S1b). Furthermore, the lattice parameter of  $(\text{Fe}_2\text{Ti}_{0.5}\text{Mn}_{0.5})_{1-\delta}\text{O}_4$  was less than that of  $(\text{Fe}_{2.5}\text{Ti}_{0.5})_{1-\delta}\text{O}_4$  (shown in Table S1) because the radius of  $\text{Mn}^{4+}$  (0.60 Å) is less than that of  $\text{Fe}^{3+}$  (0.64 Å). They both indicate that Mn cations were incorporated into the spinel structure.

After the further incorporation of V into the spinel structure, additional reflections that would indicate the presence of other crystalline vanadium oxides, such as  $\text{V}_2\text{O}_5$ ,  $\text{VO}_2$ ,  $\text{V}_2\text{O}_4$ ,  $\text{V}_2\text{O}_3$  or  $\text{FeVO}_4$ , were not present in the diffraction scan of  $(\text{Fe}_2\text{Ti}_{0.5}\text{V}_{0.5})_{1-\delta}\text{O}_4$  (shown in Fig. S1c). Furthermore, the lattice parameter of  $(\text{Fe}_2\text{Ti}_{0.5}\text{V}_{0.5})_{1-\delta}\text{O}_4$  (shown in Table S1) was less than that of  $(\text{Fe}_{2.5}\text{Ti}_{0.5})_{1-\delta}\text{O}_4$  because the radii of  $\text{V}^{4+}$  (0.63 Å) and  $\text{V}^{5+}$  (0.59 Å) are less than that of  $\text{Fe}^{3+}$  (0.64 Å). They both indicate that V cations were incorporated into the spinel structure. However, two subtle reflections centered at  $33.07^\circ$  and  $40.79^\circ$  appeared in the diffraction scan of  $(\text{Fe}_2\text{Ti}_{0.5}\text{V}_{0.5})_{1-\delta}\text{O}_4$ , which may be assigned to  $\alpha\text{-Fe}_2\text{O}_3$  (shown in Fig. S1c).

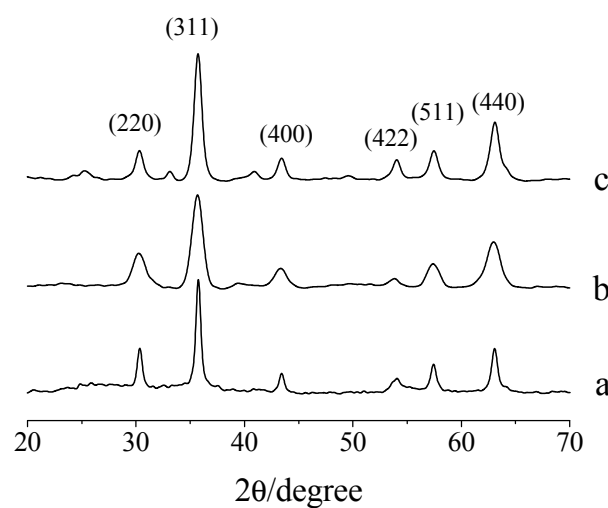


Fig. S1 XRD patterns of synthesized: (a),  $(\text{Fe}_{2.5}\text{Ti}_{0.5})_{1-\delta}\text{O}_4$ ; (b),  $(\text{Fe}_2\text{Ti}_{0.5}\text{Mn}_{0.5})_{1-\delta}\text{O}_4$ ; (c),  $(\text{Fe}_2\text{Ti}_{0.5}\text{V}_{0.5})_{1-\delta}\text{O}_4$

Crystal size was calculated with the Scherrer's equation.<sup>3</sup> As shown in Table S1, the sequence of crystal sizes of  $(\text{Fe}_{2.5}\text{Ti}_{0.5})_{1-\delta}\text{O}_4$ ,  $(\text{Fe}_2\text{Ti}_{0.5}\text{Mn}_{0.5})_{1-\delta}\text{O}_4$  and  $(\text{Fe}_2\text{Ti}_{0.5}\text{V}_{0.5})_{1-\delta}\text{O}_4$  was consistent with that of BET surfaces.

Table S1 Lattice parameter, crystal size and BET surface area of synthesized catalyst

	lattice parameter (nm)	crystal size (nm)	BET surface area (m <sup>2</sup> g <sup>-1</sup> )
(Fe <sub>2.5</sub> Ti <sub>0.5</sub> ) <sub>1-δ</sub> O <sub>4</sub>	0.8378	24	36.4
(Fe <sub>2</sub> Ti <sub>0.5</sub> Mn <sub>0.5</sub> ) <sub>1-δ</sub> O <sub>4</sub>	0.8338	11	107
(Fe <sub>2</sub> Ti <sub>0.5</sub> V <sub>0.5</sub> ) <sub>1-δ</sub> O <sub>4</sub>	0.8354	15	59.6

## 2.2 XPS

Surface information of synthesized catalysts was analyzed by XPS. XPS spectra over the spectral regions of Fe 2p, V 2p, Ti 2p, Mn 2p and O 1s were evaluated (shown in Fig. S2).

The O 1s peaks mainly centered at about 530.2 eV, as expected for transition metal oxides. Another oxygen species centered at about 531.4 eV was also observed, which was assigned to hydroxyl group (-OH).<sup>4</sup>

The Ti peaks were assigned to Ti 2p 1/2 (464.4 eV) and Ti 2p 3/2 (458.7 eV) of Ti<sup>4+</sup>.

The Fe peaks were assigned to oxidized Fe species, more likely Fe<sup>3+</sup> type species.<sup>4</sup> The binding energies centered at about 710.4 and 711.2 eV may be assigned to Fe<sup>3+</sup> cations in the spinel structure, and the binding energy centered at about 712.2 eV was ascribed to Fe<sup>3+</sup> bonded with hydroxyl groups ( $\equiv$ Fe<sup>III</sup> - OH).

The V peaks on (Fe<sub>2</sub>Ti<sub>0.5</sub>V<sub>0.5</sub>)<sub>1-δ</sub>O<sub>4</sub> were assigned to V<sup>5+</sup> (517.4 eV) and V<sup>4+</sup> (516.6 eV). XPS analysis also shows that the ratios of V<sup>5+</sup> to V<sup>4+</sup> were about 1.77 and 1.27 for (Fe<sub>2</sub>Ti<sub>0.5</sub>V<sub>0.5</sub>)<sub>1-δ</sub>O<sub>4</sub> after the thermal treatment under air at 300 °C and 400 °C, respectively. It indicates that some V<sup>5+</sup> cations in (Fe<sub>2</sub>Ti<sub>0.5</sub>V<sub>0.5</sub>)<sub>1-δ</sub>O<sub>4</sub> would be self-reduced to V<sup>4+</sup> cations to sustain the spinel structure at high temperature.<sup>2</sup>

The Mn peaks on (Fe<sub>2</sub>Ti<sub>0.5</sub>Mn<sub>0.5</sub>)<sub>1-δ</sub>O<sub>4</sub> were assigned to Mn<sup>2+</sup> (640.4 eV), Mn<sup>3+</sup> (641.4 eV) and Mn<sup>4+</sup> (642.5 eV). The percent of Mn<sup>4+</sup> on (Fe<sub>2</sub>Ti<sub>0.5</sub>V<sub>0.5</sub>)<sub>1-δ</sub>O<sub>4</sub> was about 2.4%, which was much less than that of V<sup>5+</sup> on (Fe<sub>2</sub>Ti<sub>0.5</sub>Mn<sub>0.5</sub>)<sub>1-δ</sub>O<sub>4</sub> (6.1%). Therefore, the SCR activity of (Fe<sub>2</sub>Ti<sub>0.5</sub>Mn<sub>0.5</sub>)<sub>1-δ</sub>O<sub>4</sub> was much less than that of (Fe<sub>2</sub>Ti<sub>0.5</sub>V<sub>0.5</sub>)<sub>1-δ</sub>O<sub>4</sub> at 150-300 °C.

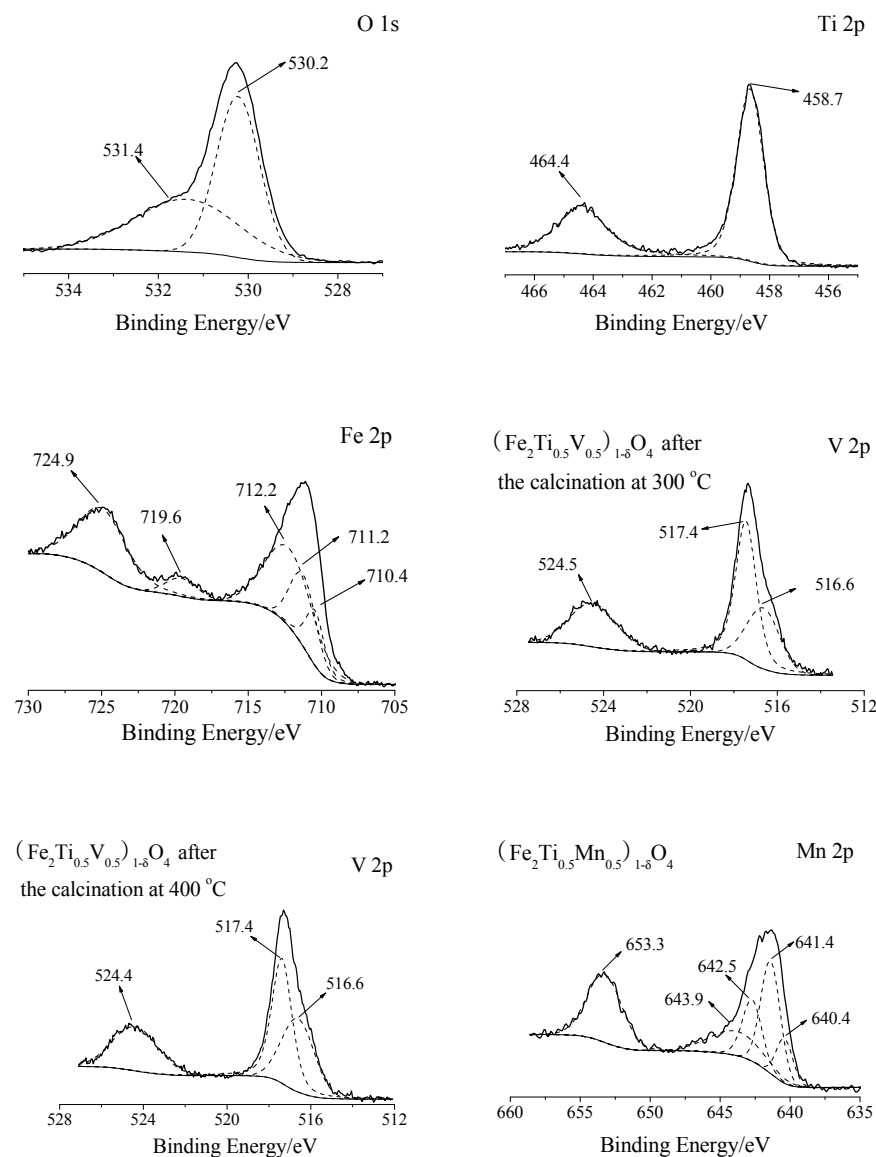


Fig. S2 XPS spectra of synthesized catalysts over the spectral regions of O 1s, Ti 2p, Fe 2p, Mn 2p and V 2p

### 2.3 Magnetization

$(\text{Fe}_2\text{Ti}_{0.5}\text{V}_{0.5})_{1-\delta}\text{O}_4$  was a super-paramagnetic catalyst with a minimized coercivity and a negligible magnetization hysteresis (shown in Fig. S3), and its saturated magnetization was about 30 emu g<sup>-1</sup>.

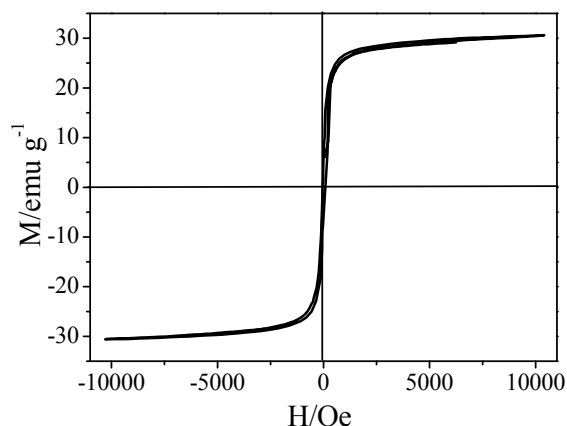


Fig. S3 Magnetization characteristics of  $(\text{Fe}_2\text{Ti}_{0.5}\text{V}_{0.5})_{1-\delta}\text{O}_4$

#### 2.4 DRIFT Study

After Fe-Ti spinel was treated with  $\text{NH}_3/\text{N}_2$  at 200 °C, four bands at 1609, 1440, 1330 and 1253  $\text{cm}^{-1}$  appeared (shown in Fig. S4a). The band at 1440  $\text{cm}^{-1}$  was assigned to ionic  $\text{NH}_4^+$  bound to the Brønsted acid sites, and the bands at 1609 and 1253  $\text{cm}^{-1}$  were attributed to coordinated  $\text{NH}_3$  bound to the Lewis acid sites. The band at 1330  $\text{cm}^{-1}$  may be attributed to the asymmetric deformation of coordinated  $\text{NH}_3$ .<sup>5</sup> The negative bands at 1373 and 1540  $\text{cm}^{-1}$  may be assigned to residual sulfate species in synthesized Fe-Ti spinel, which was covered by  $\text{NH}_3$ . After Fe-Ti spinel was treated with  $\text{NO+O}_2/\text{N}_2$  at 200 °C, three slight bands at 1624, 1450 and 1387  $\text{cm}^{-1}$  appeared (shown in Fig. S4b), which were attributed to monodentate nitrite.<sup>6</sup>

After  $\text{NO+O}_2/\text{N}_2$  passed over  $\text{NH}_3$  pretreated Fe-Ti spinel at 200 °C, the band at 1440  $\text{cm}^{-1}$  corresponding to ionic  $\text{NH}_4^+$  and the bands at 1609, 1330 and 1253  $\text{cm}^{-1}$  corresponding to coordinated  $\text{NH}_3$  both diminished (shown in Fig. S4a). Meanwhile, a new band at 1620  $\text{cm}^{-1}$  appeared. This band was assigned to adsorbed  $\text{H}_2\text{O}$ , which is the product of SCR reaction.<sup>5</sup> They both suggest that the adsorbed ammonia species on Fe-Ti spinel can react with NO. However, the bands corresponding to adsorbed nitrogen oxides can hardly be detected after  $\text{NO+O}_2/\text{N}_2$  passed over  $\text{NH}_3$  pretreated Fe-Ti spinel. After  $\text{NH}_3$  passed over  $\text{NO+O}_2$  pretreated Fe-Ti spinel, the bands at 1609, 1440, 1330 and 1253  $\text{cm}^{-1}$  corresponding to adsorbed ammonia species appeared (shown in Fig. S4b). However, the band at 1620  $\text{cm}^{-1}$  corresponding to adsorbed  $\text{H}_2\text{O}$  can hardly be detected. It suggests that the reaction between ammonia and adsorbed nitrogen oxides on Fe-Ti spinel may be neglected. Therefore, the SCR reaction over Fe-Ti spinel mainly followed the Eley-Rideal mechanism.

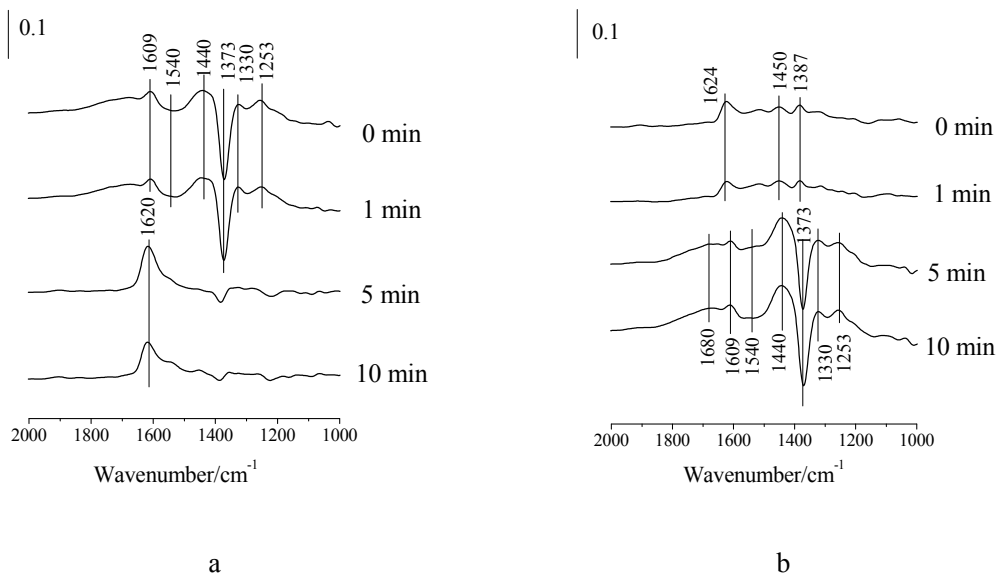
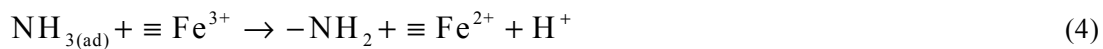


Fig. S4 (a), DRIFT spectra taken at 200 °C upon passing NO+O<sub>2</sub> over NH<sub>3</sub> presorbed Fe-Ti spinel;  
(b), DRIFT spectra taken at 200 °C upon passing NH<sub>3</sub> over NO+O<sub>2</sub> presorbed Fe-Ti spinel.

The SCR reaction over Fe-Ti spinel can be approximately described as follows:<sup>7</sup>



Reaction 3 was the adsorption of gaseous ammonia on the acid sites (i.e. Brønsted acid sites and Lewis acid sites) to form adsorbed ammonia species including ionic NH<sub>4</sub><sup>+</sup> and coordinated NH<sub>3</sub>. There is general agreement that the SCR reaction starts with the adsorption of NH<sub>3</sub>, which is very strong compared to the adsorption of NO+O<sub>2</sub> and the reaction products.<sup>8</sup> Reaction 4 was the activation of adsorbed ammonia species by Fe<sup>3+</sup> on the surface to form amide species (-NH<sub>2</sub>). Then, gaseous NO was reduced by -NH<sub>2</sub> on the surface to form N<sub>2</sub> and H<sub>2</sub>O (Reaction 5). Reaction 6 was the re-oxidation of formed Fe<sup>2+</sup>.

## Notes and references

1. S. Yang, Y. Guo, N. Yan, D. Wu, H. He, Z. Qu, C. Yang, Q. Zhou and J. Jia, *ACS Appl. Mater. Interfaces*, 2011, **3**, 209-217; S. Yang, Y. Guo, N. Yan, D. Wu, H. He, J. Xie, Z. Qu and J. Jia, *Appl. Catal. B-environ.*, 2011, **101**, 698-708.
2. S. Yang, Y. Guo, N. Yan, D. Wu, H. He, J. Xie, Z. Qu, C. Yang and J. Jia, *Chem. Commun.*, 2010, **46**, 8377-8379.
3. S. Yang, H. He, D. Wu, D. Chen, X. Liang, Z. Qin, M. Fan, J. Zhu and P. Yuan, *Appl. Catal. B-environ.*, 2009, **89**, 527-535.
4. T. Herranz, S. Rojas, M. Ojeda, F. J. Perez-Alonso, P. Tefferos, K. Pirota and J. L. G. Fierro, *Chem. Mater.*, 2006, **18**, 2364-2375; Y. Zhang, M. Yang, X. M. Dou, H. He and D. S. Wang, *Environ. Sci. Technol.*, 2005, **39**, 7246-7253.
5. G. S. Qi and R. T. Yang, *J. Phys. Chem. B*, 2004, **108**, 15738-15747.
6. K. I. Hadjiivanov, *Catal. Rev.*, 2000, **42**, 71-144.
7. S. Yang, J. Li, C. Wang, J. C. L. Ma, H. Chang, L. Chen, Y. Peng and N. Yan, *Appl. Catal. B-environ.*, 2012, doi:10.1016/j.apcatb.2012.01.001.
8. W. S. Kijlstra, D. S. Brands, H. I. Smit, E. K. Poels and A. Bliek, *J. Catal.*, 1997, **171**, 219-230.